MULTIPLE SCLEROSIS JOURNAL | MSJ

Original Research Paper

Gray matter atrophy cannot be fully explained by white matter damage in patients with MS

Jian Zhang*, Antonio Giorgio*, Claudia Vinciguerra, Maria Laura Stromillo, Marco Battaglini, Marzia Mortilla, Riccardo Tappa Brocci, Emilio Portaccio, Maria Pia Amato and Nicola De Stefano

Multiple Sclerosis Journal

1–13

DOI: 10.1177/1352458519900972

Abstract

Background: Source-based morphometry (SBM) was recently used for non-random "patterns" of gray matter (GM) atrophy or white matter (WM) microstructural damage.

Objective: To assess whether and to what extent such patterns may be inter-related in MS.

Methods: SBM was applied to images of GM concentration and fractional anisotropy (FA) in MS patients ($n=41$, median EDSS = 1) and normal controls (NC, $n=28$). The same procedure was repeated on an independent and similar data set (39 MS patients and 13 NC).

Results: We found in MS patterns of GM atrophy and reduced FA ($p<0.05$, corrected). Deep GM atrophy was mostly (70%) explained by lesion load in projection tracts and lower FA in posterior corona radiata and thalamic radiation. By contrast, sensorimotor and posterior cortex atrophy was less (50%) dependent from WM damage. All patterns correlated with EDSS (r from −0.33 to −0.56, $p<0.03$) while the only cognition-related correlation was between posterior GM atrophy pattern and processing speed ($r=0.45$, $p=0.014$). Reliability analysis showed similar results.

Conclusion: In relatively early MS, we found a close link between deep GM atrophy pattern and WM damage while sensorimotor and posterior cortex patterns were partially independent from WM damage and perhaps related to primary mechanisms. Patterns were clinically relevant.

Keywords: Multiple sclerosis, MRI, connectivity, atrophy, DTI, lesions

Date received: 19 July 2019; revised: 28 November 2019; accepted: 22 December 2019.

Correspondence to:
N De Stefano
Department of Medicine, Surgery and Neuroscience, University of Siena, Viale Bracci 2, Siena 53100, Italy.
destefano@unisi.it

Jian Zhang
Antonio Giorgio
Claudia Vinciguerra
Maria Laura Stromillo
Marco Battaglini
Riccardo Tappa Brocci
Nicola De Stefano
Department of Medicine, Surgery and Neuroscience, University of Siena, Siena, Italy

Marzia Mortilla
Anna Meyer Children's University Hospital, Florence, Italy

Emilio Portaccio
IRCCS Don Gnocchi Foundation, Florence, Italy

Maria Pia Amato
Department of NEUROFARBA, Neuroscience Division, University of Florence, Florence, Italy/IRCCS Don Gnocchi Foundation, Florence, Italy

*These authors contributed equally to the manuscript.

Introduction

Structural abnormalities, as detected by magnetic resonance imaging (MRI), are well known in multiple sclerosis (MS) brains in the form of gray matter (GM) atrophy and white matter (WM) damage.[1,2] Some studies suggested that WM damage may be spatially linked with subsequent cortical and deep GM atrophy in primary progressive and long-standing MS.[3–5] Other studies showed that most of the cortical GM atrophy may be partially independent from WM lesions in both early and progressive MS.[6,7]

Few recent studies have revealed in MS, at the level of "patterns" (i.e. co-varying structurally and/or functionally related regions of the human brain), the presence of GM atrophy[5,8] or WM microstructural damage,[9] as expressed by low fractional anisotropy (FA) on diffusion tensor imaging (DTI) data. Such patterns were detected with source-based morphometry (SBM), a novel model-free and data-driven multivariate MRI-based approach using independent component analysis (ICA) on brain images of different MRI modalities.[10] SBM allows grouping brain structural abnormalities into spatial patterns, well beyond the traditional assessment of single brain regions.[11] Such approach may thus help shed light on complex pathogenic mechanisms, including possible relationships between GM atrophy and WM microstructural damage in distinct anatomical regions of the MS brain. Given the great potential of this approach in providing new insights on this relevant issue, we used here SBM on MRI data of an MS patient cohort with relatively mild disability in order to assess whether and to what extent distinct spatial patterns of GM atrophy and WM microstructural damage exist, may be inter-related and have clinical relevance. To increase the reliability of the results, the same procedure was performed on an independent MRI data set with similar characteristics.

Table 1. Demographic, clinical, and LV characteristics of the study groups. Study and Reliability data sets were acquired, respectively, before and after MR scanner upgrade.

	Study data set (41 MS, 28 NC)	Reliability data set (39 MS, 13 NC)	*p*-value
Age (mean ± SD, years)			
MS	35.6 ± 10.4	40.7 ± 9.1	0.020[a]
NC	33.2 ± 10.0	35.6 ± 8.9	0.087[a]
p-value (MS v NC)	0.348[a]	0.257[a]	
Sex (male/female number)			
MS	13/28	13/26	0.877[b]
NC	5/23	6/7	0.057[b]
p-value (MS v NC)	0.198[b]	0.406[b]	
Disease duration (mean ± SD, years)	9.1 ± 7.0	8.0 ± 8.0	0.514[c]
EDSS (median (range))	1.5 (0–6)	1.5 (1–6.5)	0.661[c]
Cognitive impairment (yes/no) [%]	9/32 [22%]	12/27 [31%]	0.370[c]
WM LV (median (range) cm^3)	5.61 (0.30–79.05)	3.80 (0.14–31.86)	0.072[c]
Projection (median (range) cm^3)	3.4 (0.22–32.39)	2.38 (0.04–15.19)	–
Association (median (range) cm^3)	0.33 (0–9.28)	0.27 (0–2.09)	–
Commissural (median (range) cm^3)	1.19 (0.06–9.35)	0.62 (0–5.73)	–
Subcortical (median (range) cm^3)	1.74 (0.09–33.25)	1.87 (0–13.94)	–
Brainstem/cerebellar (median (range) cm^3)	0.09 (0–1.51)	0.08 (0–0.74)	–

MS: multiple sclerosis; NC: normal controls; EDSS: Expanded Disability Status Scale; WM: white matter; LV: lesion volume.
[a]Two-sample *t*-test.
[b]Chi-squared test.
[c]Mann–Whitney *U* test.

Methods

Participants

Two independent subject data sets were recruited, respectively, before and after MR scanner upgrade (Table 1): the "Study data set" of 41 MS patients and 28 normal controls (NC), and the "Reliability data set" of 39 MS patients and 13 NC. All MS patients were diagnosed with 2010 McDonald criteria[12] and had to be free from relapses and corticosteroid treatment for at least 1 month before study entry. NC were recruited among laboratory and hospital workers, had normal neurological examination and no history of neurological disorder.

In MS patients, disability was measured on the Expanded Disability Status Scale (EDSS),[13] whereas cognition was assessed by a trained and blinded neuropsychologist, using the Brief Repeatable Battery (BRB).[14] Failure of a BRB test was defined as a score <2 standard deviations from the Italian normative values[15] and cognitive impairment was defined as a failure of $\geqslant 2$ BRB tests.

The study protocol received approval from the Ethics Committee of Azienda Ospedaliera Universitaria Senese. Informed written consent was obtained from all participants before study entry in accordance with Declaration of Helsinki.

MRI data acquisition

MRI data were acquired with an eight-channel head coil on a three Tesla MR scanner (Philips Medical Systems, Best, The Netherlands) located at Meyer University Hospital, Florence. A sagittal survey image was used to identify anterior and posterior commissures. Sequences were acquired in the axial plane parallel to the bicommissural line. A dual-echo, turbo spin-echo sequence (repetition time (TR)/echo time (TE)1/TE2 = 4000/10/100 ms, voxel size = 1 × 1 × 3 mm) yielded proton density (PD) and T2-weighted (T2W) images. DTI data were an echo-planar imaging sequence (TR = 7036 ms; TE = 196 ms; voxel size = 2.5 mm^3) with 32 diffusion directions and *b*-value = 900 s/mm^2. A high-resolution T1-weighted image (T1W, TR = 10 ms, TE = 4 ms, voxel size = 1 mm^3) was also acquired for image registration, anatomical mapping and analysis of GM concentration.

Study and Reliability data sets were acquired, respectively, before and after MR scanner upgrade and using the same imaging protocol.

MRI data analysis

It was performed at the Quantitative Neuroimaging Laboratory (QNL) of the University of Siena. All images were visually assessed to rule out artifacts or incidental findings.

WM lesions. MS lesions were outlined on PD images by an experienced observer (R.T.B.), blinded to patient identity, with a semiautomated segmentation technique based on user-supervised local thresholding (Jim 6.0; Xinapse System, Leicester, UK) which allowed compute global lesion volume (LV) across brain.

Regional LV was computed using the WM parcellation map (WMPM) of a John Hopkins University (JHU) standard-space atlas (Eve Atlas, www.mristudio.org). First, for each patient, LV was calculated in each WM region (label) of the atlas by masking WMPM with the corresponding lesion mask.[16] Then, WM regions were grouped in five anatomically meaningful areas, such as projection, association, commissural, subcortical, and brainstem/cerebellar WM, in line with previous studies,[17] and for each area, LV was computed by summing the values from all corresponding WM regions (Supplementary Table 1).

Binarized lesion mask of each patient was registered onto MNI152 standard brain through tools of FSL (FMRIB Software Library, www.fmrib.ox.ac.uk/fsl) using linear registration (FLIRT (FMRIB Linear Image Registration Tool))[18] followed by nonlinear registration (FNIRT (FMRIB Non-linear Image Registration Tool)).[19] Two experienced observers (J.Z. and A.G.) independently checked all lesion masks registered onto standard brain, and an agreement was found in all cases. Finally, lesion probability map (LPM) was generated first merging and then averaging all lesion masks previously registered onto standard brain.

GM preprocessing. We followed the VBM (voxel-based morphometry) pipeline of SPM12 (Statistical Parametric Mapping, http://www.fil.ion.ucl.ac.uk/spm/). On T1W images, GM segmentation was performed using the Unified Segmentation method after "filling" hypointense lesions.[20] Then, DARTEL (Diffeomorphic Anatomical Registration using Exponentiated Lie algebra) was used to determine the nonlinear deformations for image warping and to increase the accuracy of inter-subject alignment. Finally, all GM images were spatially normalized to Montreal Neurological Institute (MNI) standard brain and smoothed with an 8-mm full width at half maximum (FWHM) Gaussian kernel, thus representing GM concentration, a proxy for GM volume.

WM preprocessing. DTI data were preprocessed through the FSL program *Eddy*, which corrects for eddy current–induced distortions, subject movement, and signal dropout. Then, we used FDT (FMRIB Diffusion Toolbox) to obtain FA images by fitting a diffusion tensor model at each voxel. All subjects' FA images were first registered onto a standard-space image (FMRIB58_FA) using FNIRT[21] and then smoothed with a 3-mm sigma (i.e. 7-mm FWHM) Gaussian kernel. For each MS patient, the information on lesion mask was incorporated into the FNIRT step in order to avoid over-distortion of lesion areas.

SBM of GM and FA images. Following the original pipeline,[10] analyses were performed on images of GM concentration[11] (i.e. without modulation by Jacobian determinant) and FA of the Study data set using GIFT (Group ICA of FMRI Toolbox; http://mialab.mrn.org/software/gift/).

The number of independent components (IC) (i.e. patterns) was automatically estimated with the "minimum description length" criterion through a neural network algorithm (Infomax). The statistical reliability of these patterns was tested using ICASSO (software for investigating the reliability of ICA estimates by clustering and visualization), which repeated estimation 10 times with different initial conditions and bootstrapped data sets. For each time of estimation, a set of IC was obtained from bootstrapped samples of the image series. Each bootstrapped data set consisted of about one-third of the total images in the series.

Patterns were arrayed into two matrices. The first matrix was a "mixing matrix" (subject-by-pattern), which indicates the loading coefficient of each subject for each pattern. The value of the subject-wise loading coefficient represents the corresponding GM/FA pattern (i.e. source) and can be viewed as the degree to which a pattern is present in a subject. A lower loading coefficient of the GM and FA patterns represents, respectively, GM atrophy and microstructural damage along WM tracts. The second matrix was a "source matrix" (pattern-by-GM/FA voxels), which reflects the relationship between the pattern and the GM/FA voxels.

Statistical analysis. Differences between MS and NC were tested, using the mixing matrix's loading coefficients of each pattern, with a general linear model, adjusted for age and sex. Statistical threshold was $p < 0.05$, false discovery rate (FDR)-corrected for multiple comparisons.[22]

In order to extract vectors (i.e. variables) for subsequent multivariate regression models, the source matrix of each pattern showing group difference was converted into Z scores and thresholded > 3, thus creating a "pattern mask." Then, the mean of the voxels within the "pattern mask" was calculated for each patient, generating an $N_{subj} \times 1$ vector for each pattern, in line with a recent pipeline.[23]

Spearman coefficient, FDR-corrected, was used to investigate correlation of GM and FA pattern measures (i.e. vectors) with clinical measures (EDSS and BRB tests) and to compute correlations between measures of GM (i.e. vectors of GM atrophy patterns) and WM (i.e. vectors of FA patterns, global and regional LV), FDR-corrected for multiple comparisons.

We then used stepwise multivariate linear regression analyses, in which vectors of each GM atrophy pattern were treated as dependent variable while FA pattern vectors, global LV (log-transformed to allow normal distribution), and regional LV (Z-transformed to allow normal distribution) were considered as independent variables. The combination of measures of WM macro- and microstructural damage able to best predict each pattern of GM atrophy in the Study data set was tested using the following equation

$$\text{GM atrophy Pattern} = \text{Constant} + \beta_1 \times (\text{Regional LV}) + \beta_2 \times (\text{FA Pattern})$$

Finally, in order to increase reliability of the results, the same SBM procedure was repeated on an independent data set of MS patients and NC with similar characteristics. First, SBM was run on GM and FA images of the Reliability data set using the same setting as the Study data set. Second, the multivariate regression model (i.e. beta-coefficients) best predicting each GM atrophy pattern of the Study data set was applied to the Reliability data set. Pearson correlations between true and predicted values of each GM atrophy pattern were assessed.

p-value < 0.05 was set as significant for all analyses, performed with R software (https://www.r-project.org/).

Results

Clinical, demographic, and LV characteristics of the study groups

There was no age and sex difference between MS and NC for both Study ($p = 0.348$ and $p = 0.198$, respectively) and Reliability ($p = 0.257$ and $p = 0.406$, respectively) data sets. In the comparison between Study and Reliability data sets, there was no age and sex difference for NC ($p = 0.087$ and $p = 0.057$, respectively) and MS patients did not differ for sex ($p = 0.877$), disease duration ($p = 0.514$), EDSS ($p = 0.661$), proportion of cognitive impairment ($p = 0.370$), and LV ($p = 0.072$). Data are summarized in Table 1.

GM patterns

Six GM patterns were automatically detected across brain of the Study data set.

GM atrophy ($p < 0.05$, FDR-corrected) was found in MS patients compared to NC for Pattern-1 ("deep GM pattern": caudate and thalamus), Pattern-2 ("sensorimotor GM pattern": paracingulate gyrus, precuneous cortex, precentral gyrus, supplementary motor cortex, superior frontal gyrus, and postcentral gyrus), and Pattern-4 ("posterior GM pattern": inferior temporal gyrus, occipital fusiform gyrus, lingual gyrus, posterior cingulate, and precuneus cortex) (Figure 1(a) and (b), Table 2).

No significant group differences were found for Pattern-3 (inferior frontal gyrus, pars opercularis), Pattern-5 (lateral occipital cortex, parahippocampal gyrus), and Pattern-6 (cerebellar cortex).

FA patterns

Four FA patterns were automatically detected across brain of the Study data set.

Lower FA ($p < 0.05$, FDR-corrected) in MS than NC was found for FA Pattern-2 (corticospinal tract (CST, internal capsule and brainstem) and splenium of the corpus callosum (sCC), both mainly in the normal appearing WM) and FA Pattern-4 (posterior thalamic radiation (PTR) and corona radiata (PCR), overlapping with WM lesions) (Figure 1(a) and (b), Table 3).

No significant group difference was found for FA Pattern-1 (superior corona radiata). FA Pattern-3 was visually identified as noise and thus discarded.

Correlation of patterns of GM atrophy and reduced FA with clinical measures

All patterns of GM atrophy and reduced FA correlated with EDSS (r from -0.33 to -0.56, $p < 0.03$) while, for cognition tests, the only significant correlation

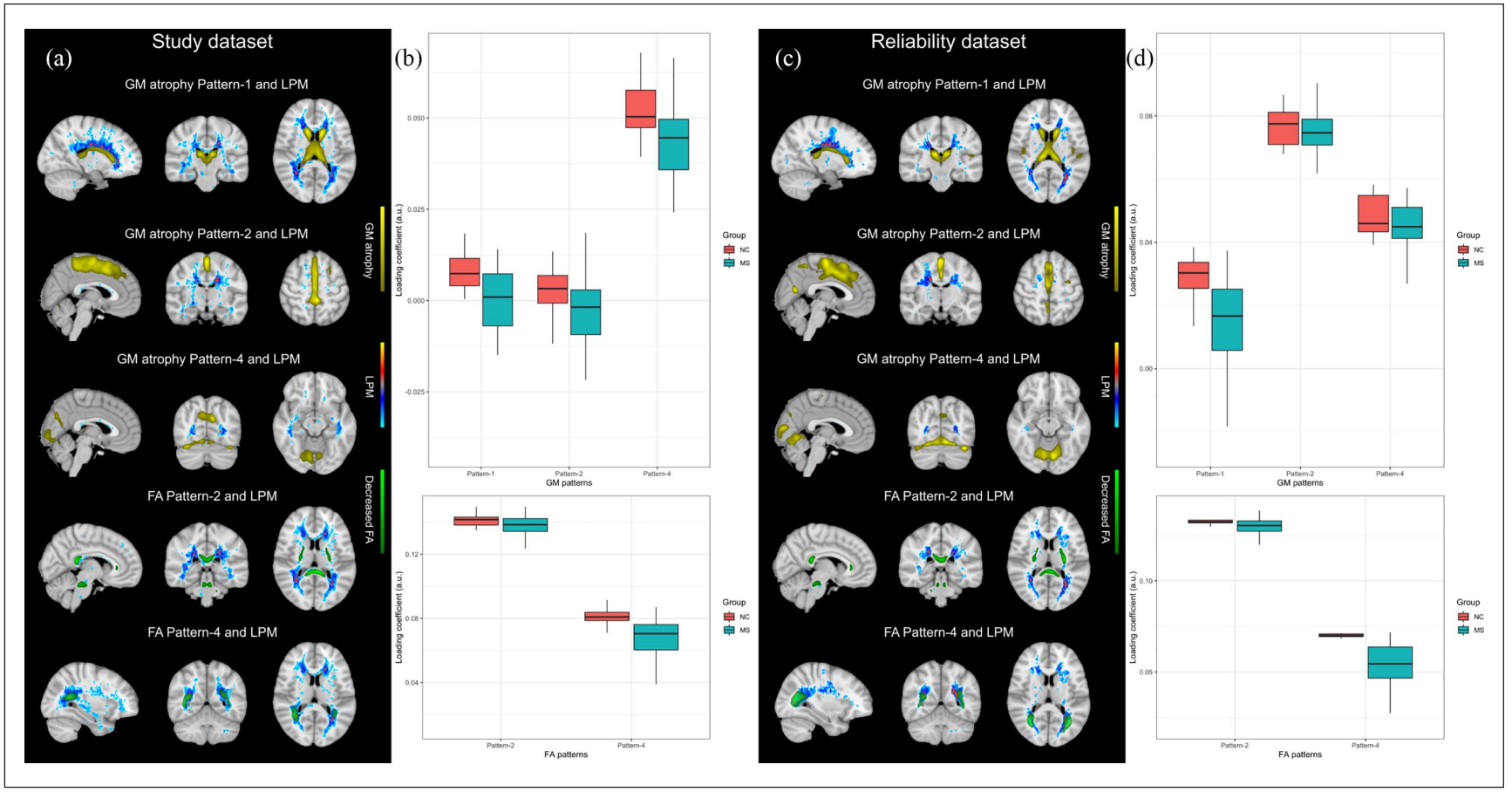

Figure 1. Significant patterns of GM atrophy (in yellow, $Z > 3$) and WM microstructural damage (i.e. decreased FA) (in green, $Z > 3$) in our group of MS patients with relatively mild disability compared to NC and corresponding box plots of loading coefficients are shown for the Study (a and b) and Reliability (c and d) data sets. Lesion probability map (in light-blue to yellow, range: 1%–46% for both data sets) is also shown to assess the spatial relationship between lesions and significant patterns. Background image is the MNI152 standard brain, in radiological orientation.

a.u.: arbitrary unit.

Table 2. Patterns of GM atrophy ($p < 0.05$, FDR-corrected) in MS patients with relatively mild disability compared to NC in the Study data set.

GM atrophy pattern	Brain region (local maxima)	Side	MNI (*x, y, z*)	*Z*-value	*p*-value of pattern
1	Caudate	R	12, 18, 10	8.8	0.006
		L	−12, 14, 12	9.1	
	Thalamus	L	−8, −18, 16	8.1	
		R	10, −20, 16	7.7	
2	PCG	R	2, 12, 48	7.2	0.014
	PreCC	L	−6, −36, 48	4.9	
	PreG	L	−2, −38, 54	7.7	
	SMC	M	0, 6, 54	6.9	
	PreCC	R	2, −38, 56	6.9	
	SFG	R	4, 14, 56	5.7	
	PosG	L	−4, −44, 66	5.5	
		R	6, −46, 66	4.6	
4	ITG	L	−46, −54, −26	5.6	0.001
	OFG	R	18, −80, −18	4.7	
	LG	R	10, −68, −12	4.5	
	PosC	M	0, −63, 15	3.6	
	PreCC	L	−10, −72, 28	5.3	
		R	8, −72, 34	4.6	

Within each pattern, brain regions were ordered by increasing coordinates on the *z*-axis.
GM: gray matter; FDR: false discovery rate; L: left; R: right; PCG: paracingulate gyrus; PreCC: precuneous cortex; PreG: precentral gyrus; SMC: supplementary motor cortex; SFG: superior frontal gyrus; PosG: postcentral gyrus; ITG: inferior temporal gyrus; OFG: occipital fusiform gyrus; LG: lingual gyrus; PosC: posterior cingulate.

Table 3. Patterns of decreased FA ($p < 0.05$, FDR-corrected), reflecting microstructural damage along WM tracts, in MS with relatively mild disability compared to NC in the Study data set.

FA pattern	Brain region (local maxima)	Side	MNI (*x, y, z*)	*Z*-value	*p*-value of pattern
2	CST	L	−23, −15, 9	3.6	0.023
	Splenium of CC	L	−6, −39, 15	4.8	
		R	10, −40, 17	4.7	
4	PTR/OR	L	−38, −51, 4	3.9	<0.001
		R	33, −50, 15	5.5	
	PCR	L	−27, −46, 22	4.4	

Within each pattern, brain regions were ordered by increasing coordinates on the *z*-axis.
FA: fractional anisotropy; FDR: false discovery rate; L: left; R: right; CST: corticospinal tract; CC: corpus callosum; PTR: posterior thalamic radiation; OR: optic radiation; PCR: posterior corona radiata.

was found between GM atrophy Pattern-4 and Symbol Digit Modalities Test (SDMT) ($r = 0.45$, $p = 0.014$) (Table 4).

Correlation between patterns of GM atrophy and WM damage measures

The anatomical relationship between GM atrophy patterns and lesions across brain (LPM) is shown in Figure 1. The three GM atrophy patterns showed a moderate-to-close correlation with the two FA patterns (Figure 2) and with global and supratentorial LV (Spearman correlation in Table 5).

The stepwise multivariate linear regression analysis (Multivariate regression model in Table 5) showed that GM atrophy Pattern-1 was highly explained ($R^2 = 0.723$, adjusted (for the number of predictors) $R^2 = 0.709$, $p < 0.001$) by both LV along WM projection tracts and

Table 4. Correlation between patterns of GM atrophy and reduced FA and clinical measures in the Study data set.

	EDSS		SDMT	
	Rho	*p*-value[a]	*Rho*	*p*-value[a]
GM Pattern-1	−0.46	0.004	0.13	0.410
GM Pattern-2	−0.33	0.035	0.24	0.173
GM Pattern-4	−0.49	0.003	0.45	0.014
FA Pattern-2	−0.56	0.001	0.23	0.173
FA Pattern-4	−0.43	0.006	0.27	0.173

GM: gray matter; FA: fractional anisotropy; EDSS: Expanded Disability Status Scale; SDMT: Symbol Digit Modalities Test.
[a]FDR (false discovery rate)-corrected.

FA Pattern-4; GM atrophy Pattern-2 was moderately explained ($R^2=0.522$, adjusted $R^2=0.510$, $p<0.001$) by FA Pattern-4; finally, GM atrophy Pattern-4 was moderately explained ($R^2=0.604$, adjusted $R^2=0.584$, $p<0.001$) by both LV in subcortical WM and FA Pattern-4.

Generalizability of SBM and multivariate regression model

When the analysis was performed on the Reliability data set, we found high spatial similarity with corresponding patterns of the Study data set (Figure 1 (a) and (c) Supplementary Tables 2 and 3). As shown in Figure 3, all predicted values of GM atrophy patterns in the Reliability data set showed significant correlations with corresponding true vales of the Study data set (GM atrophy Pattern-1: $r=0.77$, $p<0.001$; GM atrophy Pattern-2: $r=0.60$, $p<0.001$; GM atrophy Pattern-4: $r=0.58$, $p<0.001$), suggesting good generalizability of the multivariate regression models.[23]

Discussion

In this study, we sought to assess in MS patients with relatively mild disability whether and to what extent distinct anatomical non-random "patterns" of GM atrophy and WM microstructural damage may be inter-related. Furthermore, the clinical relevance of such patterns was investigated. For this purpose, we applied to MRI data SBM, a novel model-free and data-driven multivariate approach using spatial ICA.

Non-random patterns of GM atrophy and WM microstructural damage

Most of the GM regions of our atrophy patterns were found in a recent longitudinal SBM study on MS,[8] whose atrophy patterns indeed included caudate and thalamus (GM atrophy Pattern-1), precuneous cortex, precentral gyrus, supplementary motor cortex (GM atrophy Pattern-2), inferior temporal gyrus, and lingual gyrus (GM atrophy Pattern-4). Moreover, our atrophy pattern in the posterior GM was in line with another recent SBM study on long-standing MS, where a pattern of cortical thinning similarly mapped on lingual gyrus and posterior cingulate cortex.[5]

As for FA patterns, decreased FA in CST, sCC (FA Pattern-2), and PTR (FA Pattern-4) was also found in a recent SBM study on secondary progressive MS.[9] However, in that study, sCC and CST mapped in separate patterns, thus demonstrating that WM microstructural damage may be differently organized in MS groups with different disability.

Despite similarities, differences across SBM studies exist and may be related to patient populations as well as methodologies, including MR field strength, type of SBM, and pattern detection (automated vs predefined). Interestingly, however, in this study, the three significant GM atrophy patterns and the two FA patterns in the Study data set were confirmed, with high spatial similarity, on the Reliability data set, suggesting that such patterns are stable and consistent when using the same methodology.

Atrophy in caudate and thalamus, expressed here as deep GM pattern (GM atrophy Pattern-1), was recently shown to drive disability worsening in MS[24] and is likely due to demyelination, inflammation, axonal injury, iron deposition, and oxidative stress.[25] Atrophy in sensorimotor cortex (GM atrophy Pattern-2), despite relatively mild disability of our MS group, was previously found associated with motor dysfunction.[26–29] Atrophy in posterior cortex (GM atrophy Pattern-4) was similarly found in a recent SBM study,[5] which linked it to impairment in information processing speed.

Reduced FA in our MS group with relatively mild disability was found in CST and sCC (FA Pattern-2), in line with a previous tract-based spatial statistics study where both WM tracts resulted associated with EDSS in MS patients with mild disability.[30] Moreover, reduced FA was found in PCR and PTR (FA Pattern-4). The former, containing descending projection fibers of the CST, subserves motor function to the lower limbs. Altered diffusion in PCR is in line with a recent study on pediatric-onset MS in the early adulthood with no or minimal disability[31] and highlights that, even at this disease stage, there is already damage along a WM tract clinically eloquent for ambulation, which indeed represents the major contributor to

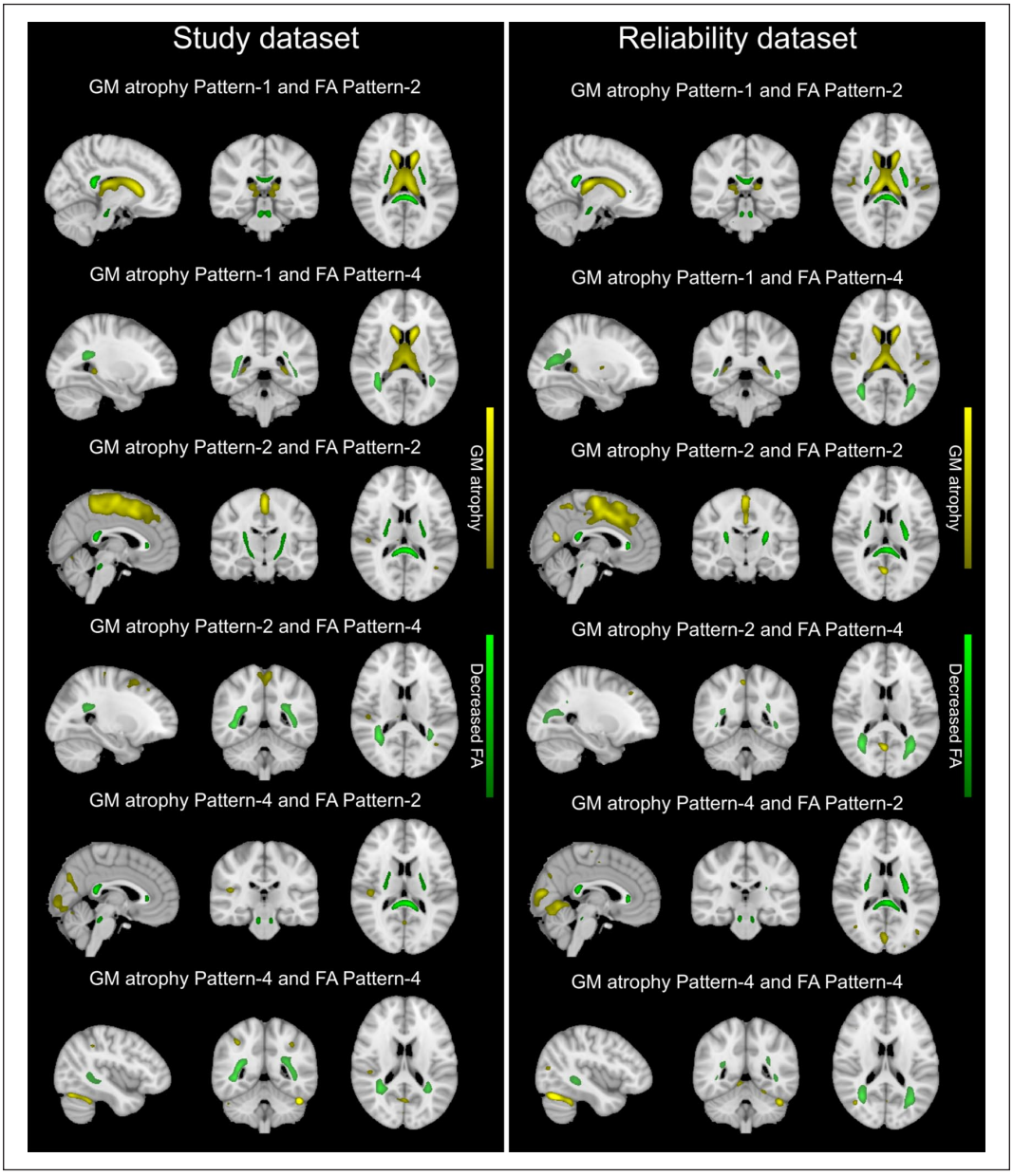

Figure 2. Spatial relationship between patterns of GM atrophy (in yellow, $Z > 3$) and WM microstructural damage (i.e. decreased FA) (in green, $Z > 3$) in our group of MS patients with relatively mild disability for the Study (left panel) and Reliability (right panel) data sets. Background image is the MNI152 standard brain, in radiological orientation.

EDSS. The latter, also containing projection fibers, is an important cognition-related WM tract in MS, showing close associations with processing speed and visual working memory.[32]

Association between patterns of GM atrophy and reduced FA with clinical measures

All GM and FA patterns showed a low-to-moderate correlation with EDSS. Such results are in line with previous studies showing that EDSS correlated with atrophy in regions of sensorimotor cortex,[5,27] deep and posterior GM.[24,33] Likewise, WM tracts of our FA patterns were singularly reported in previous studies to correlate with EDSS.[34,35]

Of note, FA Pattern-2 (CST and sCC, mainly in the normal appearing WM) showed higher correlation with disability than FA Pattern-4 (PTR and PCR, mostly overlapping with lesions), supporting the clinical relevance of microstructural damage beyond macroscopic WM lesions.[2]

Table 5. Correlation between patterns of GM atrophy and measures of WM damage and stepwise multivariate linear regression models in the Study data set.

Spearman correlation	GM atrophy Pattern-1		GM atrophy Pattern-2		GM atrophy Pattern-4	
	Rho	*p*-value[a]	*Rho*	*p*-value[a]	*Rho*	*p*-value[a]
FA Pattern-2	0.54	<0.001	0.57	<0.001	0.65	<0.001
FA Pattern-4	0.67	<0.001	0.70	<0.001	0.73	<0.001
Global LV	−0.77	<0.001	−0.66	<0.001	−0.64	<0.001
Projection LV	−0.73	<0.001	−0.60	<0.001	−0.61	<0.001
Association LV	−0.59	<0.001	−0.55	<0.001	−0.65	<0.001
Commissural LV	−0.67	<0.001	−0.52	<0.001	−0.56	<0.001
Subcortical LV	−0.71	<0.001	−0.63	<0.001	−0.65	<0.001
Brainstem/Cerebellar LV	−0.33	0.038	−0.37	0.018	−0.55	<0.001
Multivariate regression model						
	R^2=0.723*[a], Adj. R^2=0.709, RMSE=0.044		R^2=0.522*[a], Adj. R^2=0.510, RMSE=0.053		R^2=0.604*[a], Adj. R^2=0.584, RMSE=0.045	
	Beta coefficient		Beta coefficient		Beta coefficient	
Constant	0.178		0.048		0.432	
Predictors						
FA Pattern-4	0.566**		1.005*		0.524**	
Projection LV	−0.041**		–		–	
Subcortical LV	–		–		0.524**	

GM: gray matter; FA: fractional anisotropy; Adj.: adjusted for the number of predictors, RMSE: root mean square error; LV: lesion volume.
[a]FDR (false discovery rate)-corrected.
*$p < 0.001$.
**$p < 0.05$.

The only significant correlation with cognition tests was found between GM atrophy Pattern-4 and impairment in information processing speed, highlighting the key role of posterior GM atrophy for deficits of information processing.[5]

Association between patterns of GM atrophy and measures of WM damage

The three significant GM atrophy patterns showed a moderate-to-close relationship with FA, particularly in the posterior WM regions overlapping with lesions (FA Pattern-4). Moreover, they also correlated with both global and regional LV. Most of these associations with supratentorial LV were particularly close for caudate and thalamus atrophy (GM atrophy Pattern-1), thus supporting the idea that WM lesions are an important contributor to atrophy in these structures.[4] Indeed, in both Study and Reliability data sets, the multivariate regression model showed that atrophy in caudate and thalamus (GM atrophy Pattern-1) was highly explained, in the order of 70%, by lesion load along WM projection tracts and decreased FA in PCR and PTR (FA Pattern-4). This finding highlights the importance for deep GM atrophy of WM damage, in terms of both macrostructural damage along WM tracts clinically eloquent for motor function and WM microstructural damage in posterior regions mostly overlapping with lesions.

Interestingly, however, cortical atrophy (GM atrophy Pattern-2 and Pattern-4) was less explained by WM damage (in the order of about 50% in the two data sets), thus indicating that this may be, at least in part, independent from WM damage in MS patients with relatively mild disability. The remaining variance might be explained by other pathological processes, including meningeal inflammatory infiltrates, recently shown to act as independent factor for cortical atrophy beyond WM lesions,[6,32] and the possible upstream sensorimotor GM atrophy in presence of spinal cord pathology,[36,37] which however was not investigated in our study.

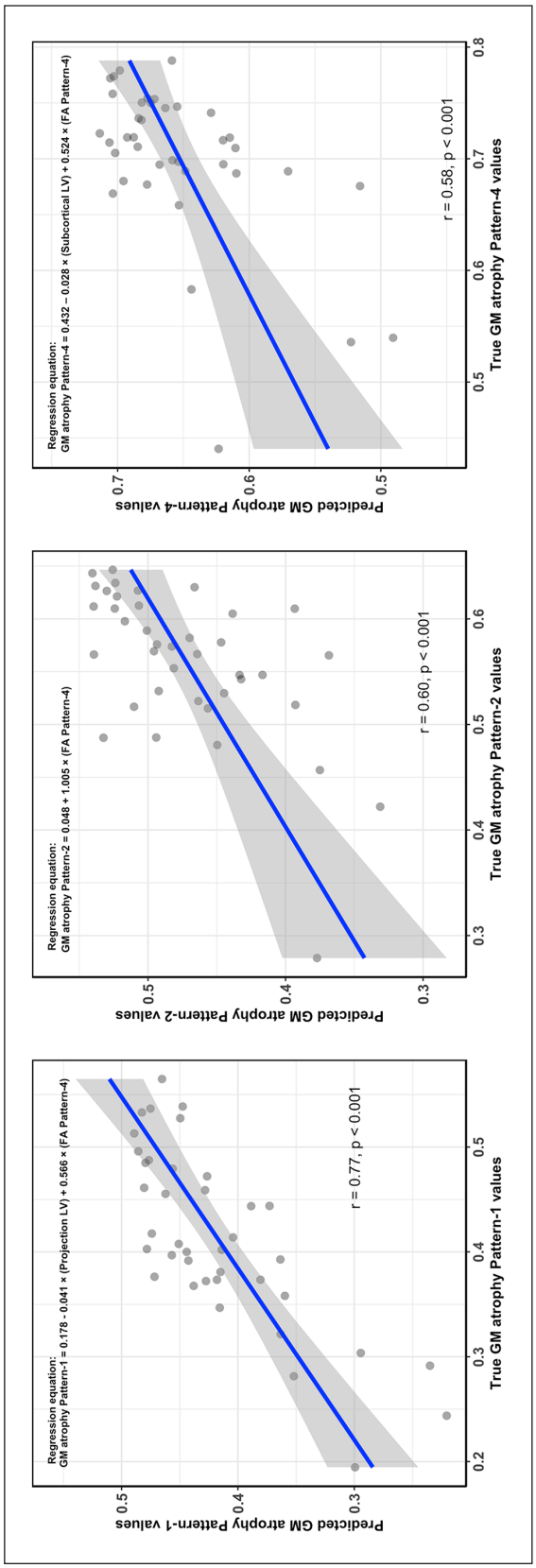

Figure 3. Scatter plots showing correlation between predicted values of GM atrophy pattern in the Reliability data set and corresponding true values obtained from multivariate regression analyses in the Study data set.

Strengths and limitations

Important limitations of this study lie in the cross-sectional design and the relatively small sample size. Moreover, we are aware that in MS volumetric measurement of posterior GM regions, which are part of our GM Pattern-4, may be more dependent, unlike other GM regions, on the analysis method used, as recently demonstrated.[38] Atrophy in these posterior GM regions may be related to damage in the visual system, and indeed, we found a close correlation with FA Pattern-4, which included optic radiations.

Compared to VBM, surface-based methods may potentially yield a better registration quality.[5] However, they do not include in the default pipeline important brain structures for MS such as deep GM regions and cerebellum[5] and do not automatically estimate the number of IC in SBM, thus potentially introducing a bias. We are aware that VBM-based nonlinear registration may, to some extent, be affected by the presence of brain atrophy. Reassuringly, a careful check of all registered images allowed us to rule out the presence of clear misregistrations affecting the creation of brain patterns. Moreover, the great reproducibility of our results in two independent data sets with similar characteristics strongly increases the confidence in the robustness of the study.

SBM was applied here to assess patterns of GM atrophy and WM microstructural damage and their interrelation. This approach has shown some strengths, as it seems to ideally overcome some limitations of graph theory–based structural network analysis regarding inappropriately defined "nodes" through atlas-based parcellation, arbitrarily thresholded correlation matrix, and high degree of abstraction of network matrix, whose complex measures are simply represented by numbers.[10,39] Moreover, ICA-based analyses, including SBM, turn out be more straightforward to interpret compared to canonical correlation analysis (CCA) due to the clear distinction of correlation coefficients,[40] adjustment for the nuisance effect of the dependence between variables[41] and automated estimation of the IC number.[42] However, SBM performs a separate assessment of the GM atrophy and FA patterns and the subsequent post hoc analyses of correlation and multivariate regression. Future studies should assess the pathogenic relevance of the direct combination or "fusion" of such patterns using upfront imaging analysis methods.

In conclusion, using cutting-edge MR-based methodology, we provide here evidence of a close link between WM damage and deep GM atrophy. By contrast, cortical atrophy seems to be, at least in part, independent from WM damage. This could be explained by a primary cortical neurodegeneration and perhaps related to other primary mechanisms, including meningeal inflammation. Moreover, all altered patterns had clinical relevance, showing correlation with physical disability, whereas only posterior GM atrophy pattern showed correlation with reduced cognitive performance, at the level of information processing speed.

Acknowledgements

We wish to thank Maria Pia Sormani (University of Genoa) for statistical advice.

Declaration of Conflicting Interests

The author(s) declared the following potential conflicts of interest with respect to the research, authorship, and/or publication of this article: J.Z., A.G., C.V., M.L.S., M.B., M.M., and R.T.B. report no discloses. E.P. serves on a scientific advisory board for Biogen-Idec, Merck Serono, and Bayer. He received honoraria and research grants from Merck Serono, Biogen Idec, Bayer Schering, Novartis, Teva, and Genzyme. M.P.A. is member of Advisory Boards for Biogen, Merck, Teva, Novartis, Sanofi Aventis, Genzyme, Almirall, and Roche. She received honoraria for speaking from Biogen, Merck, Novartis, Teva, Genzyme, Almirall, and Sanofi Aventis. She is member of Editorial Board and Associate Editor of BMC Neurology Member of the Editorial Board of *Multiple Sclerosis Journal*. She has received research grants from Biogen, Merk, Bayer, Sanofi Aventis, and Teva. N.D.S. has received honoraria from Biogen-Idec, Genzyme, Merck Serono, Novartis, Roche, and Teva for consulting services, speaking, and travel support. He serves on advisory boards for Merck Serono, Novartis, Biogen-Idec, Roche, and Genzyme, and he has received research grant support from the Italian MS Society.

Funding

The author(s) disclosed receipt of the following financial support for the research, authorship, and/or publication of this article: The study was supported by a grant of the Italian Ministry of Health for Young Researchers (GR-2011-02352201).

ORCID iD

Jian Zhang https://orcid.org/0000-0001-8820-3248

Supplemental Material

Supplemental material for this article is available online.

References

1. Geurts JJG, Calabrese M, Fisher E, et al. Measurement and clinical effect of grey matter pathology in multiple sclerosis. *Lancet Neurol* 2012; 11(12): 1082–1092.
2. Filippi M, Preziosa P and Rocca MA. Brain mapping in multiple sclerosis: Lessons learned about the human brain. *NeuroImage* 2019; 190: 32–45.
3. Bodini B, Chard D, Altmann DR, et al. White and gray matter damage in primary progressive MS: The chicken or the egg? *Neurology* 2016; 86(2): 170–176.
4. Steenwijk MD, Daams M, Pouwels PJW, et al. What explains gray matter atrophy in long-standing multiple sclerosis. *Radiology* 2014; 272(3): 832–842.
5. Steenwijk MD, Geurts JJG, Daams M, et al. Cortical atrophy patterns in multiple sclerosis are non-random and clinically relevant. *Brain* 2016; 139(Pt 1): 115–126.
6. Kawachi I and Lassmann H. Neurodegeneration in multiple sclerosis and neuromyelitis optica. *J Neurol Neurosurg Psychiatry* 2017; 88(2): 137–145.
7. Zurawski J, Lassmann H and Bakshi R. Use of magnetic resonance imaging to visualize leptomeningeal inflammation in patients with multiple sclerosis: A review. *JAMA Neurol* 2017; 74(1): 100–109.
8. Bergsland N, Horakova D, Dwyer MG, et al. Gray matter atrophy patterns in multiple sclerosis: A 10-year source-based morphometry study. *Neuroimage Clin* 2018; 17: 444–451
9. Meijer KA, Cercignani M, Muhlert N, et al. Patterns of white matter damage are non-random and associated with cognitive function in secondary progressive multiple sclerosis. *Neuroimage Clin* 2016; 12(Supplement C): 123–131.
10. Xu L, Groth KM, Pearlson G, et al. Source-based morphometry: The use of independent component analysis to identify gray matter differences with application to schizophrenia. *Hum Brain Mapp* 2009; 30(3): 711–724.
11. Gupta CN, Calhoun VD, Rachakonda S, et al. Patterns of gray matter abnormalities in schizophrenia based on an international mega-analysis. *Schizophr Bull* 2015; 41(5): 1133–1142.
12. Polman CH, Reingold SC, Banwell B, et al. Diagnostic criteria for multiple sclerosis: 2010 Revisions to the McDonald criteria. *Ann Neurol* 2011; 69(2): 292–302.
13. Kurtzke JF. Rating neurologic impairment in multiple sclerosis: An expanded disability status scale (EDSS). *Neurology* 1983; 33(11): 1444–1452.
14. Rao SM. *A manual for the brief repeatable battery of neuropsychological tests in multiple sclerosis*. Milwaukee, WI: Medical College of Wisconsin, 1990.
15. Amato MP, Portaccio E, Goretti B, et al. The Rao's Brief Repeatable Battery and Stroop test: Normative values with age, education and gender corrections in an Italian population. *Mult Scler* 2006; 12(6): 787–793.
16. Oishi K, Faria A, Jiang H, et al. Atlas-based whole brain white matter analysis using large deformation diffeomorphic metric mapping: Application to normal elderly and Alzheimer's disease participants. *NeuroImage* 2009; 46(2): 486–499.
17. Hua K, Zhang J, Wakana S, et al. Tract probability maps in stereotaxic spaces: Analyses of white matter anatomy and tract-specific quantification. *NeuroImage* 2008; 39(1): 336–347.
18. Jenkinson M and Smith S. A global optimisation method for robust affine registration of brain images. *Med Image Anal* 2001; 5(2): 143–156.
19. Andersson JL, Jenkinson M, Smith S, et al. *Non-linear registration, aka spatial normalisation* (Internet). FMRIB technical report TR07JA2 2007, https://www.fmrib.ox.ac.uk/analysis/techrep/tr07ja2/tr07ja2.pdf (accessed 7 July 2016).
20. Battaglini M, Jenkinson M and De Stefano N. Evaluating and reducing the impact of white matter lesions on brain volume measurements. *Hum Brain Mapp* 2012; 33(9): 2062–2071.
21. Smith SM, Jenkinson M, Johansen-Berg H, et al. Tract-based spatial statistics: Voxelwise analysis of multi-subject diffusion data. *NeuroImage* 2006; 31(4): 1487–1505.
22. Winkler AM, Webster MA, Brooks JC, et al. Non-parametric combination and related permutation tests for neuroimaging. *Hum Brain Mapp* 2016; 37(4): 1486–1511.
23. Sui J, Qi S, van Erp TGM, et al. Multimodal neuromarkers in schizophrenia via cognition-guided MRI fusion. *Nat Commun* 2018; 9(1): 3028.
24. Eshaghi A, Prados F, Brownlee WJ, et al. Deep gray matter volume loss drives disability worsening in multiple sclerosis. *Ann Neurol* 2018; 83(2): 210–222.
25. Haider L, Simeonidou C, Steinberger G, et al. Multiple sclerosis deep grey matter: The relation between demyelination, neurodegeneration, inflammation and iron. *J Neurol Neurosurg Psychiatry* 2014; 85(12): 1386–1395.
26. Sailer M, Fischl B, Salat D, et al. Focal thinning of the cerebral cortex in multiple sclerosis. *Brain* 2003; 126(Pt 8): 1734–1744.
27. Bodini B, Khaleeli Z, Cercignani M, et al. Exploring the relationship between white matter and gray matter damage in early primary progressive multiple

sclerosis: An in vivo study with TBSS and VBM. *Hum Brain Mapp* 2009; 30(9): 2852–2861.

28. Prinster A, Quarantelli M, Lanzillo R, et al. A voxel-based morphometry study of disease severity correlates in relapsing–remitting multiple sclerosis. *Mult Scler* 2010; 16(1): 45–54.
29. Narayana PA, Govindarajan KA, Goel P, et al. Regional cortical thickness in relapsing remitting multiple sclerosis: A multi-center study. *Neuroimage Clin* 2012; 2: 120–131.
30. Giorgio A, Palace J, Johansen-Berg H, et al. Relationships of brain white matter microstructure with clinical and MR measures in relapsing-remitting multiple sclerosis. *J Magn Reson Imaging* 2010; 31(2): 309–316.
31. Giorgio A, Zhang J, Stromillo ML, et al. Pronounced structural and functional damage in early adult pediatric-onset multiple sclerosis with no or minimal clinical disability. *Front Neurol* 2017; 8: 608.
32. Yu HJ, Christodoulou C, Bhise V, et al. Multiple white matter tract abnormalities underlie cognitive impairment in RRMS. *NeuroImage* 2012; 59(4): 3713–3722.
33. Eshaghi A, Marinescu RV, Young AL, et al. Progression of regional grey matter atrophy in multiple sclerosis. *Brain* 2018; 141: 1665–1677.
34. Welton T, Kent D, Constantinescu CS, et al. Functionally relevant white matter degradation in multiple sclerosis: A tract-based spatial meta-analysis. *Radiology* 2014; 275(1): 89–96.
35. Enzinger C, Barkhof F, Ciccarelli O, et al. Nonconventional MRI and microstructural cerebral changes in multiple sclerosis. *Nat Rev Neurol* 2015; 11(12): 676–686.
36. Freund P, Weiskopf N, Ashburner J, et al. MRI investigation of the sensorimotor cortex and the corticospinal tract after acute spinal cord injury: A prospective longitudinal study. *Lancet Neurol* 2013; 12(9): 873–881.
37. Meyer CE, Gao JL, Cheng Oberoi MR, et al. Axonal damage in spinal cord is associated with gray matter atrophy in sensorimotor cortex in experimental autoimmune encephalomyelitis. *Mult Scler*. Epub ahead of print 7 March 2019. DOI: 10.1177/1352458519830614.
38. Popescu V, Schoonheim MM, Versteeg A, et al. Grey matter atrophy in multiple sclerosis: Clinical interpretation depends on choice of analysis method. *PLoS ONE* 2016; 11(1): e0143942.
39. Smith SM. The future of FMRI connectivity. *NeuroImage* 2012; 62(2): 1257–1266.
40. Calhoun VD and Sui J. Multimodal fusion of brain imaging data: A key to finding the missing link(s) in complex mental illness. *Biol Psychiatry Cogn Neurosci Neuroimaging* 2016; 1(3): 230–244.
41. Lee TW, Girolami M and Sejnowski TJ. Independent component analysis using an extended Infomax algorithm for mixed subgaussian and supergaussian sources. *Neural Comput* 1999; 11(2): 417–441.
42. Li Y-O, Adali T and Calhoun VD. Estimating the number of independent components for functional magnetic resonance imaging data. *Hum Brain Mapp* 2007; 28(11): 1251–1266.